

HIGH POWER, HIGH FREQUENCY TRAVELING WAVE HETEROJUNCTION PHOTOTRANSISTORS WITH INTEGRATED POLYIMIDE WAVEGUIDE

D. C. Scott, D. P. Prakash, H. Erlig, D. Bhattacharya, M. Ali, and H. R. Fetterman
 Electrical Engineering Department, University of California, Los Angeles, CA 90095-1594 USA

M. Matloubian
 Hughes Research Laboratories, Malibu, CA 90265 USA

Abstract

A high power, high speed phototransistor has been demonstrated using a traveling wave structure with an integrated polyimide optical waveguide. In our configuration, optical power transfer is distributed along the length of the device via leaky mode coupling of light from the polyimide waveguide to the active region of the phototransistor. The traveling wave electrode design allows for an electrically long structure while maintaining high bandwidths. Due to the increased absorption volume, the optical power handling capabilities of the TW-HPT are improved over that of conventional lumped element HPT detectors. The experimental results show no compression of the fundamental at 60GHz up to 50mA of DC photocurrent.

Introduction

One of the major commercial incentives driving research in photonics is the microwave fiber optic link. A typical link consists of a laser source, an external modulator, the fiber optic transmission medium, and an optical detector. High frequency optical detectors are one of the primary components that dictate the system performance of the fiber optic link. In order to reduce the RF insertion loss, increase the spurious free dynamic range, and increase the signal-to-noise ratio of the link, the photodetector needs to be able to handle high optical powers [1]. As an example, the RF gain of a link containing a Mach-Zehnder modulator is given by the expression

$$\text{RF Gain} = \left(\frac{\pi q G P_o}{V_\pi h \nu} \right)^2 (R_{\text{mod}} \cdot R_l) \quad (1)$$

where V_π is the voltage required to change the Mach-Zehnder modulator from the on to the off state and R_{mod} is the input resistance of the modulator. P_o is the optical power incident on the detector, R_l is the load resistance that the detector drives, G is the optical gain of the detector, q is the electronic charge, and $h\nu$ is the photon energy. From equation (1), we find that the link gain is a strong function of the optical power and improves with increasing P_o . Also, the link gain is shown to improve with increasing optical gain. As such, Heterojunction Phototransistors (HPTs) which exhibit optical gain via transistor action have a large advantage over *p-i-n* or *MSM* photodiodes for use in

photonic links. Although much work has been done on high speed phototransistors [2], a classic design conflict exists between the simultaneous optimization of high frequency performance and optical coupling efficiency. Lumped element HPTs with RC bandwidth limitations need to be scaled down in size to minimize capacitances for high speed operation. This results in poor optical coupling efficiency and reduced absorption volume. In addition, these small devices tend to saturate at low input optical power levels because of the small absorption volume. The saturation of the photocurrent under intense illumination is primarily caused by the electric field screening effect due to the high concentration of photo-generated carriers. The saturation power can be increased by enlarging the effective absorption volume thereby reducing the concentration of photo-generated carriers. However, this would result in a decrease in electrical bandwidth due to an increase in the RC time constant of the device.

In an attempt to overcome these problems, we propose to utilize the traveling wave concepts that have been implemented so successfully in optical modulator technology and extend these concepts to HPT detectors. A schematic diagram of our Traveling Wave Heterojunction Phototransistor (TW-HPT) is shown in figure 1. In our approach, we define a leaky-mode polyimide waveguide on top of the active region of the HPT. Intensity modulated light is coupled into the polyimide waveguide and leaks into the HPT's active region along the length of the device due to the fact that the index of refraction of the semiconductor is higher than that of the polyimide. The metal pads of the HPT are coplanar waveguide with the center line contacting the emitter and the ground plane contacting the collector. The base is floating. The coplanar waveguide is designed to have a characteristic impedance of 50Ω . A microwave signal is generated on the transmission line as light is absorbed along the length of the detector. The ultimate bandwidth limitation of such a device is based on the velocity mismatch between the optical wave and the induced electrical microwave although other factors have been shown by Lin, et. al. [3] to contribute to bandwidth degradation.

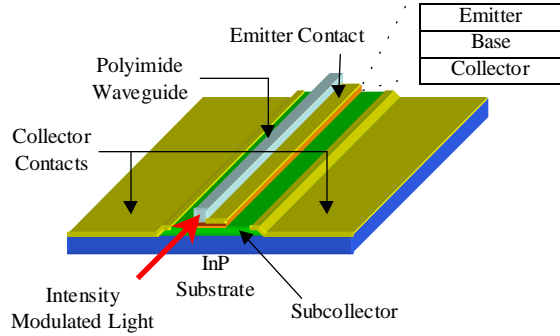


Figure 1. Schematic diagram of the TW-HPT. Polyimide waveguide is defined on top of the active region of an HPT. The HPT's electrodes are coplanar waveguide with a characteristic impedance of 50Ω .

Nonetheless, the traveling wave configuration allows for additional degrees of freedom in the optimization of device speed and optical power transfer/saturation by permitting the design of electrically long devices.

Traveling wave detectors were originally proposed by H. F. Taylor, *et. al.* [4] and much work has been done in *p-i-n* and *MSM* device structures [3,5]. Unlike *MSM* or *p-i-n* traveling wave implementations, the TW-HPT provides gain at the IF frequencies. In addition, the previously investigated devices in [3,5] utilized a semiconductor optical waveguide that was defined by the layer structure. Thus, the design of the optical waveguide and the design of the device are intimately related by the growth of the wafer. In such a configuration, any changes in the design of the optical waveguide requires regrowth of the wafer. The integration of polyimide as the optical waveguide allows for changes in the optical power transfer to the HPT without the need to change the layer structure of the wafer. As a result, the layer structure can be optimized for device performance while the optical power transfer can be tailored by independently adjusting the dimensions of the polyimide waveguide.

Due to the integration of the polyimide waveguide and the HPT in the traveling wave configuration, power saturation effects are greatly improved because the absorption of the incident light signal is distributed along the entire length of the device. The rate at which light couples to the device and is absorbed can be described by an effective absorption coefficient. To investigate the leaky mode coupling concept, we used a simulation program by Rsoft, Inc., called BeamProp which is based on the beam propagation method. We simulated structures consisting of polyimide waveguides of various thicknesses on top of InGaAs to extract the effective absorption coefficient at an optical wavelength of $1.3\mu m$. The index of refraction of the polyimide waveguide and InGaAs was 1.52 and 3.368, respectively. The absorption coefficient for bulk InGaAs at an optical wavelength of $1.3\mu m$ was taken to be

$1.5 \times 10^4 cm^{-1}$. Figure 2 shows the simulated effective optical absorption coefficient as a function of polyimide waveguide thickness. These simulations demonstrate the large range of control over the effective absorption coefficient that can be achieved. This leads to design flexibility for varying the length of the detector and still maintaining optimal optical absorption.

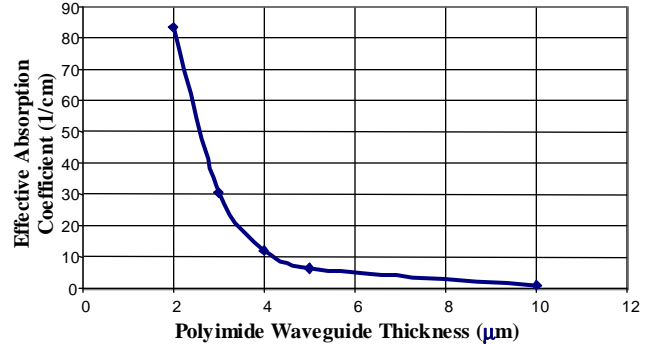


Figure 2. Effective absorption coefficient as a function of the polyimide waveguide thickness. The effective absorption coefficient can be varied over a large range by changing the thickness of the polyimide waveguide.

Device Design

The top view layout for the TW-HPT is shown in figure 3. The layer structure is a typical HBT design consisting of a 600\AA base with a graded base-emitter junction. The polyimide optical waveguide is defined on top of the emitter and lies in the gap between the center electrode and the ground plane. Since the core size for single mode fiber at an optical wavelength of $1.3\mu m$ is approximately $9\mu m$, we chose the lateral dimension of the polyimide waveguide to be $10\mu m$. The dimensions of the coplanar waveguide were chosen to be compatible with the mesa structure and to provide low propagation losses while maintaining a 50Ω characteristic impedance. The center electrode width was $20\mu m$ and the gap between the center electrode and the ground planes was $15.11\mu m$. The center electrode overlaps the side of the device mesa which is protected by SiO_2 such that the electrode only makes contact to the top emitter layer. A second set of devices were also fabricated in which the center electrode shorts the emitter to the base to form a diode structure. We will refer to this device as TW-Diode. This will allow us to compare the output response of the TW-HPT which has optical gain to a TW-Diode with exactly the same dimensions. The coplanar waveguide flares out to dimensions that are compatible with $100\mu m$ pitch coplanar probes while maintaining a 50Ω characteristic impedance. The optical input is orthogonal to the active device region and offset to ensure that the light that is detected is from the leaky mode coupling via the polyimide waveguide. The 90° bend in the optical waveguide has a radius of $0.5mm$. The optical absorption

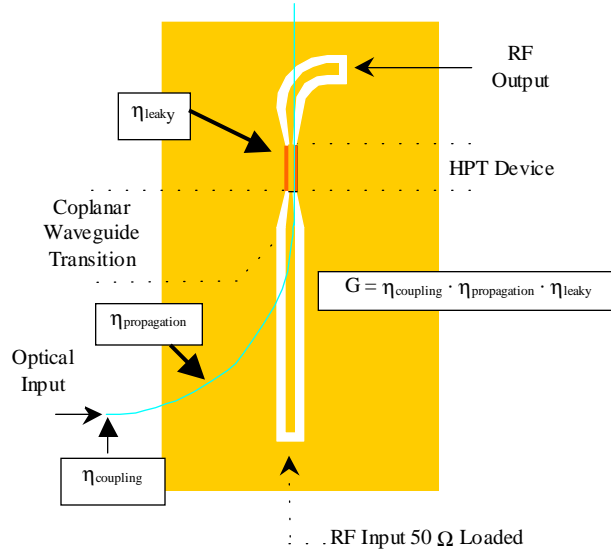


Figure 3. TW-HPT device layout.

interaction length between the waveguide and the HPT device was varied from $20\mu m$, $200\mu m$, to $2000\mu m$. The RF input of the device can be terminated by a 50Ω load or can be open circuited. The thickness of the polyimide waveguide was measured to be $7.5\mu m$.

Experimental Results

The DC optical responses of the TW-HPT and TW-Diode are shown in figures 4(a) and 4(b), respectively. A bias voltage of $V_{ce} = 1.5V$ was applied to all devices.

Comparing the two figures, it is evident that the transistor action of the TW-HPT dramatically increases the sensitivity of the optical response. The optical gain G is as high as 13.5 for the $2mm$ long TW-HPT as opposed to $G = 0.374$ for the diode. For a given optical power of $2.8mW$, the $2mm$ long diode photocurrent is $0.8mA$ but the corresponding transistor photocurrent is $40mA$ which is 50 times larger. In all cases the induced photocurrent increases linearly with increasing optical power indicating that the devices are not saturating.

By measuring the photocurrent as a function of device length for a given optical power, we can estimate the input optical coupling efficiency. This is most easily accomplished with the diode since the transistor gain can vary from device to device. The results for the TW-Diode are shown in figure 5 for three different input optical powers. The solid lines are a theoretical fit to the measured data based on the equation

$$I_{ph} = \frac{qG}{hv} P_o \quad (2)$$

I_{ph} is the optically generated portion of the output current, P_o is the incident optical power, q is the electronic charge,

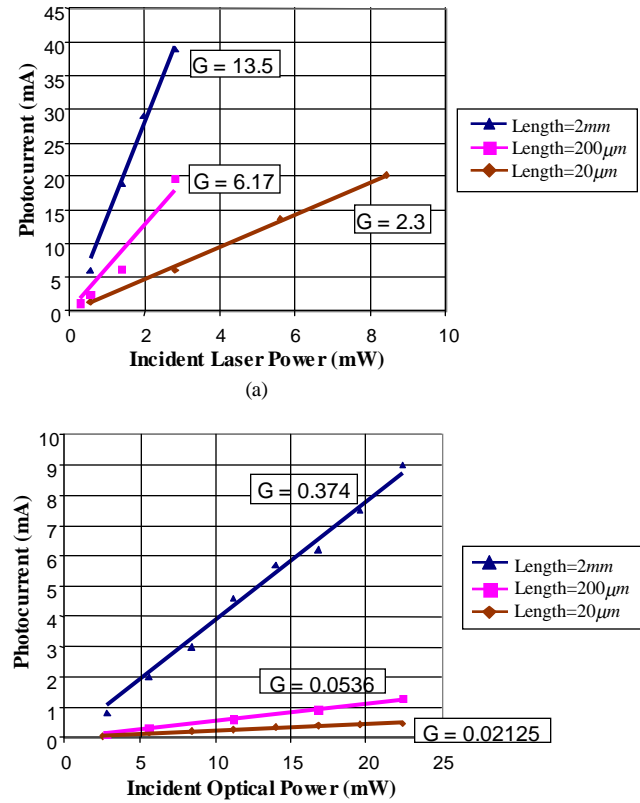


Figure 4. DC optical response of the (a) TW-HPT and (b) TW-Diode.

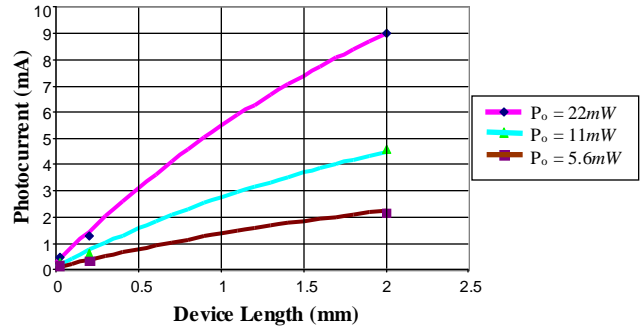


Figure 5. Photocurrent as a function of TW-Diode device length for three different incident optical powers. The solid lines are the theoretical fit to the data.

$h\nu$ is the energy of the incident photons and G is the optical gain. The optical gain can be broken up into separate efficiency factors that describe the different mechanisms for light loss and light absorption. From figure 3, we can divide optical gain into three factors

$$G = \eta_{coupling} \cdot \eta_{propagation} \cdot \eta_{leaky} \quad (3)$$

where $\eta_{coupling}$ is the input coupling loss between the optical fiber and the polyimide waveguide, $\eta_{propagation}$ is the propagation loss from the optical input of the device to the active region, and η_{leaky} is the amount of light absorption that occurs in the active region via the leaky mode coupling mechanism. $\eta_{propagation}$ is difficult to estimate so we will combine $\eta_{propagation}$ with $\eta_{coupling}$ and define this as the total input coupling loss prior to the active region of the device. From this point on, $\eta_{coupling}$ will represent both the input coupling loss and the propagation loss. η_{leaky} represents the amount of light that will be absorbed in the active region of the device via leaky mode coupling and can be written mathematically as

$$\eta_{leaky} = 1 - e^{-\alpha_{op} l} \quad (4)$$

where α_{op} is the effective absorption coefficient which is determined by the thickness of the polyimide waveguide and l is the length of the active region. Plugging in equations (3) and (4) into (2) we obtain

$$(I_c)_{opt} = \frac{qP_o}{hv} \eta_{coupling} (1 - e^{-\alpha_{op} l}) \quad (5)$$

Given that our polyimide waveguide thickness was measured to be $7.5\mu m$, the effective optical absorption coefficient given by our simulations is taken to be $\alpha_{op} = 4\text{cm}^{-1}$ (See figure 2). We can now fit equation (5) to the measured data of the $20\mu m$, $200\mu m$, and 2mm long TW-Diodes as shown in figure 5 and determine the value for $\eta_{coupling}$ as 0.7. Thus, based on these measurements the input coupling efficiency is estimated to be 70%.

The optical power saturation measurements for the TW-HPTs were made at 60GHz using two diode pumped Nd:YAG lasers in an optical mixing configuration at a wavelength of $1.3\mu m$. The results are presented for the $200\mu m$ long device since this seemed to exhibit the best trade-off between device length and performance. The results for the TW-HPT were compared to a lumped-element HPT that was fabricated with a similar layer structure and had an emitter area of $8 \times 8\mu m$. The displayed data in figure 6 shows that the lumped-element HPT output signal begins to saturate at a photocurrent of 8mA whereas the $200\mu m$ long TW-HPT shows no signs of saturation up to 50mA . The power handling ability of the TW-HPT is far superior to that of the lumped-element HPT due to the distributed nature of the optical absorption via the leaky mode configuration.

Conclusion

We experimentally measured the optical response of the TW-HPT and demonstrated high optical gains with input optical coupling efficiencies of 70%. A $200\mu m$ long TW-HPT exhibited no output power compression up to 50mA of DC photocurrent at an operating frequency of 60GHz . We envision widespread applications of the high power, high

frequency TW-HPT in future photonic and optoelectronic integrated circuits.

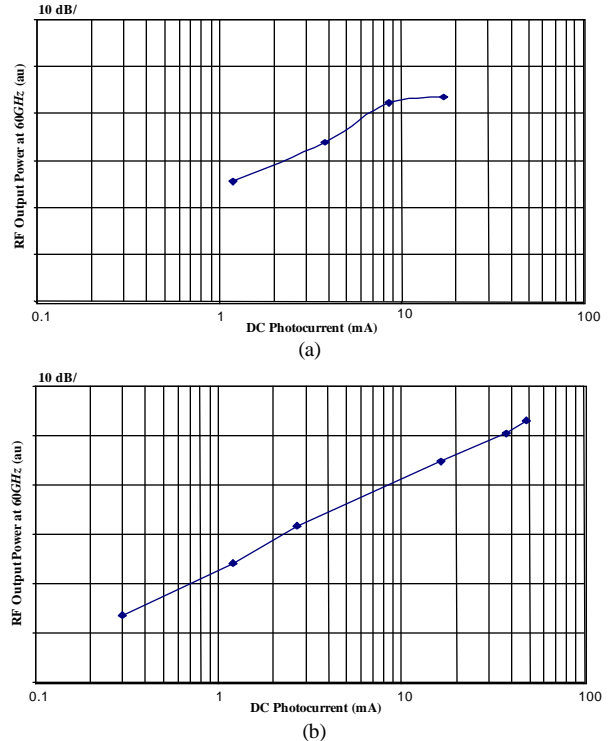


Figure 6. Optical power saturation at 60GHz for (a) lumped element HPT and (b) $200\mu m$ long TW-HPT.

References

- [1] L. Lembo, F. Alvarez, D. Lo, C. Tu, P. Wisseman, C. Zmudzinski, and J. Brock, "Optical electroabsorption modulators for wideband, linear, low-insertion loss photonic links," *SPIE*, vol. 2481, pp. 185-196, 1996.
- [2] S. Chandrasekhar, M. K. Hoppe, A. G. Dentai, C. H. Joyner, and G. J. Qua, "Demonstration of enhanced performance of an InP/InGaAs heterojunction phototransistor with a base terminal," *IEEE Electron Dev. Lett.*, vol. 12, no. 10, 1991.
- [3] L. Y. Lin, M. C. Wu, T. Itoh, T. A. Vang, R. E. Muller, D. L. Sivco, and A. Y. Cho, "High-power high-speed photodetectors-design, analysis, and experimental demonstration," *IEEE Trans. Microwave Theory and Tech.*, vol. 45, no. 8, pp. 1320-1331, 1997.
- [4] H. F. Taylor, O. Eknayan, C. S. Park, K. N. Choi, and K. Chang, "Traveling wave photodetectors," in *Proc. SPIE, Optoelectronic signal processing for phased-array antennas II*, vol. 1217, pp. 59-63, 1990.
- [5] V. M. Hietala, A. Vawter, T. M. Brennan, and B. E. Hammons, "Traveling-wave photodetectors for high-power, large-bandwidth applications," *IEEE Trans. on Microwave Theory and Tech.*, vol. 43, no. 9, pp. 2291-2297, 1995.